INFECTION AND IMMUNITY, Feb. 2006, p. 1255–1265 Vol. 74, No. 2
0019-9567/06/$08.00+0 doi:10.1128/IAI.74.2.1255–1265.2006

The Established Intimin Receptor Tir and the Putative Eucaryotic Intimin Receptors Nucleolin and β1 Integrin Localize at or near the Site of Enterohemorrhagic *Escherichia coli* O157:H7 Adherence to Enterocytes In Vivo

James F. Sinclair,[1] Evelyn A. Dean-Nystrom,[2] and Alison D. O'Brien[1]*

Department of Microbiology and Immunology, Uniformed Services University of the Health Sciences, Bethesda, Maryland,[1] and Pre-Harvest Food Safety and Enteric Disease Research Unit, National Animal Disease Center, Agricultural Research Service, U.S. Department of Agriculture, Ames, Iowa[2]

Received 14 July 2005/Returned for modification 29 September 2005/Accepted 26 November 2005

For enterohemorrhagic *Escherichia coli* (EHEC) O157:H7 to adhere tightly to the intestinal epithelium and produce *a*ttach and *e*fface (A/E) lesions, the organism must express the adhesin intimin and insert the bacterially encoded *t*ranslocated *i*ntimin *r*eceptor Tir into the plasma membrane of the host enterocyte. Additionally, some reports based on tissue culture experiments indicate that intimin has affinity for the eucaryotic proteins nucleolin and β1 integrin. To address the potential biological relevance of these eucaryotic proteins in the infection process in vivo, we sought to compare the proximity of Tir, nucleolin, and β1 integrin to regions of EHEC O157:H7 attachment in intestinal sections from three different inoculated animals: piglets, neonatal calves, and mice. Piglets and neonatal calves were chosen because intimin-mediated adherence of EHEC O157:H7 and subsequent A/E lesion formation occur at high levels in these animals. Mice were selected because of their ease of manipulation but only after we first demonstrated that in competition with the normal mouse gut flora, an EHEC O157:H7 strain with a nonpolar deletion in the intimin gene was cleared faster than strains that produced wild-type or hybrid intimin. In all three animal species, we noted immunostained Tir beneath and stained nucleolin closely associated with adherent bacteria in intestinal sections. We also observed immunostained β1 integrin clustered at locations of bacterial adherence in porcine and bovine tissue. These findings indicate that nucleolin and β1 integrin are present on the luminal surface of intestinal epithelia and are potentially accessible as receptors for intimin during EHEC O157:H7 infection.

Intimin is an outer membrane adhesin expressed by certain bacterial strains that form *a*ttach and *e*fface (A/E) lesions on the host intestinal epithelium (9). The best studied of these are enteropathogenic *Escherichia coli* (EPEC) and enterohemorrhagic *E. coli* (EHEC) strains. *Citrobacter rodentium*, a natural pathogen of mice, also produces this phenotype (35). The gene for intimin production is contained on a pathogenicity island known as the *l*ocus of *e*nterocyte *e*ffacement (LEE) (22). Also contained on LEE is the gene for the *t*ranslocated *i*ntimin *r*eceptor (Tir) (25). The protein Tir is injected into host cell cytoplasm through a type III secretion system (20). The interaction between intimin expressed on the surface of the bacterium and Tir in the host cell triggers the formation of an actin-rich pedestal that firmly anchors the bacterium to the host cell surface (13).

Intimin was first described by Jerse and Kaper as an essential protein for EPEC colonization of human intestinal epithelial cells (21) and, subsequently, was shown to be necessary for EHEC O157:H7 colonization and disease pathogenicity in neonatal calves (6) and newborn piglets (7, 29). The importance of intimin to bacterial colonization of animals is also suggested by the isolation of intimin-positive *E. coli* from a variety of species that include not only cattle (2) and pigs (31) but also rabbits (22) and dogs (3), as well as isolation of intimin-positive *C. rodentium* from mice (35). Intimin also appears to contribute to EHEC O157:H7 persistence in adult cattle and sheep (5) but not older pigs (23). In spite of the apparent importance of the *eae* intimin gene among certain intestinal bacteria, the sequences of *eae* loci from various animal isolates differ significantly (28). Indeed, at least 14 separate intimin subtypes have been proposed based on these sequence variations (1, 4, 39). All intimin subtypes bind the cognate Tir molecule, but different subtypes may have variable interactions with eucaryotic cells (11). EPEC, *C. rodentium*, and EHEC O157:H7 produce the subtypes intimin-α, intimin-β, and intimin-γ, respectively.

Although intimin is required for EHEC O157:H7 infection in some species, mice inoculated with EHEC O157:H7 do not become sick (24). In fact, they show no symptoms of the diarrheal disease or kidney damage that are hallmarks of EHEC infection in humans. Even when the normal enteric flora is eliminated by pretreatment with antibiotic, EHEC O157:H7-inoculated mice generally appear healthy (38). Judge et al. have demonstrated that mice are persistently colonized at low levels with EHEC O157:H7 in a process that requires intimin (24). One of our goals was to investigate the adherence of EHEC O157:H7 to mouse intestinal epithelium. The modest level of EHEC O157:H7 colonization in mice made it difficult to locate adherent bacteria in tissue sections from inoculated

* Corresponding author. Mailing address: Department of Microbiology and Immunology, Uniformed Services University of the Health Sciences, 4301 Jones Bridge Rd., Bethesda, MD 20814. Phone: (301) 295-3419. Fax: (301) 295-3773. E-mail: aobrien@usuhs.mil.

TABLE 1. Bacterial strains and plasmids used for this study

Strain or plasmid	Description	Reference or source
EHEC O157:H7 strains		
86-24	Isolated in 1986 from a patient in Seattle, Wash.	32
86-24 Str^r	Streptomycin-resistant strain of 86-24	30
86-24*eae*Δ10 Str^r	Streptomycin-resistant, intimin deletion strain	29
Plasmids		
pEB310	Encodes the *eae* gene of EHEC O157:H7	29
pIntgbhyb	Encodes the hybrid γβ *eae* gene	This study
pBluescriptKS−	*eae* gene negative-control plasmid	Stratagene

intestine, and for this reason we sought a means to increase the number of EHEC present in the intestine. Conversely, mice infected with *C. rodentium* are colonized at high levels and present symptoms of disease, e.g., colonic hyperplasia characterized by infiltration of lymphocytes into the infected intestine (35). Intimin-β produced by *C. rodentium* induces the hyperplasia seen during infection, a condition that may be critical to establishing a high level of bacterial colonization in mice (17). Hartland et al. have shown that mouse intestinal colonization by *C. rodentium* was reduced when the extracellular domain of intimin normally expressed by the bacteria was replaced with that of intimin type γ produced by EHEC O157:H7 (16). Therefore, we reasoned that replacement of the extracellular domain of intimin-γ with that of intimin-β might increase the level of EHEC O157:H7 colonization in mice. Here we present data for the infection of mice with a strain of EHEC O157:H7 that produces this hybrid intimin molecule.

The finding that bacterially encoded Tir is necessary for tight adherence to the host cell has sparked some debate as to whether a eucaryotic intimin receptor(s) is also involved in bacterial adherence (11). Several observations suggest that there are interactions between intimin and a eucaryotic receptor when Tir is not present (15, 33, 34). First, invasin, an adhesin encoded by *Yersinia* species that shares significant homology with intimin (22), mediates phagocytic uptake of the bacterium by the host cell (19). Interaction between invasin and β1 integrin on the host cell surface triggers cytoskeletal rearrangements within the cell (18). Because of the sequence similarity between intimin and invasin, the association between EPEC intimin-α and β1 integrin was examined in studies by Frankel and colleagues (10). They found that intimin-α did bind to β1 integrin, though this interaction was apparently not required for intimin-mediated adherence of EPEC to human epithelial cell culture (27). Second, we have reported that the intimin subtypes expressed by EHEC O157:H7, EPEC O127:H6, and *C. rodentium* each bind to the eucaryotic protein nucleolin (36) and that nucleolin appears to be involved in the initial adherence of intimin-presenting bacteria in a human epithelial cell tissue culture model. We also reported that nucleolin and Tir compete for a single binding region on intimin, though Tir has a 10-fold-greater affinity (37). In that same tissue culture model study, we noted that nucleolin localized around the site of adherence, while Tir was found beneath adherent bacteria (37). In spite of these observations of a potential eucaryotic receptor for intimin, there is little, if any, direct evidence available to support or refute the hypothesis that such a receptor(s) is involved in intimin-mediated adherence in vivo. Therefore, the major goal of this study was to use immunofluorescence methods to examine and compare the locations of β1 integrin and nucleolin in fixed tissue from infected animals to determine if these putative eucaryotic intimin receptors were present at the site of bacterial adherence. In addition, we assessed the distribution of Tir in EHEC O157:H7-infected tissues, because, in spite of the large body of in vitro evidence to support the hypothesis that Tir accumulates in the pedestals of EHEC O157:H7 attached to the host intestine, there is very little in vivo data to support this assumption (8).

MATERIALS AND METHODS

Strains and plasmids. The bacterial strains and plasmids used for this study are listed in Table 1. EHEC O157:H7 strain 86-24, isolated from an outbreak in Seattle, WA (32), was obtained from Phillip Tarr. Construction of the intimin deletion strain EHEC O157:H7 86-24*eae*Δ10 and the plasmid pEB310, which contains the *eae* gene of EHEC O157:H7, were described previously (29). EHEC O157:H7 strains 86-24 and 86-24*eae*Δ10 were selected for resistance to streptomycin (Str^r) as described previously (29, 30). A hybrid intimin consisting of the intracellular and transmembrane domains of EHEC O157:H7 with the extracellular domain of *C. rodentium* intimin was generated as follows. The *eae* gene of *C. rodentium* was cloned by PCR into an expression vector to generate plasmid pIntb936, as detailed elsewhere (37). Plasmids pEB310 and pIntb936 were cut with the restriction enzymes SalI and HindIII (New England Biolabs, Beverly, MA). The 5′ fragment of *C. rodentium eae* was ligated to the 3′ portion of the EHEC O157:H7 *eae* gene in pEB310 to generate plasmid pIntgbhyb. EHEC O157:H7 strain 86-24*eae*Δ10 Str^r was transformed separately with pEB310 or pIntgbhyb to produce complemented strains that expressed full-length EHEC O157:H7 intimin or the hybrid intimin. Expression of intimin in the transformed strains was confirmed with Western blot analysis of bacterial protein extracts separated by polyacrylamide gel electrophoresis. The capacity of the full-length intimin-expressing or hybrid intimin-expressing EHEC O157:H7 strain 86-24*eae*Δ10 Str^r transformants to adhere to HEp2 cells was verified by previously published methods (12). EHEC O157:H7 86-24*eae*Δ10 Str^r was also transformed with plasmid pBluescriptKS− (Stratagene, La Jolla, CA) to provide an intimin-negative control strain that, as expected, did not adhere to HEp2 cells. All three transformed strains were resistant to both ampicillin and streptomycin, and there were no differences observed in the growth rates of these strains when propagated in LB broth (data not shown).

Mouse infection. (i) Infection of normal mice. The method used for infection of normal mice has been described previously (24). Briefly, 6-week-old female BALB/c mice (Charles Rivers Laboratories, Wilmington, MA) were fasted for 12 h prior to infection with 100 μl of a bacterial suspension that contained approximately 10^9 CFU of an EHEC O157:H7 strain suspended in a sterile solution of 50% glucose (Sigma, Saint Louis, MO). Six mice were fed intimin-positive EHEC O157:H7 86-24 Str^r strains, while five mice were fed the intimin-negative strain 86-24*eae*Δ10 Str^r. Mice from each group were housed in a single cage but separated for fecal pellet collection. Feces were collected from the mice on subsequent days (up to day 18) following bacterial inoculation. Pellets were weighed and homogenized in sterile phosphate-buffered saline (PBS) with a volume corresponding to 10 times the weight of the pellets to yield a 1-to-10 dilution of fecal homogenate. Serial dilutions of the fecal homogenates were plated onto sorbitol-MacConkey agar (Difco Laboratories, Sparks, MD) that contained streptomycin (USB Corporation, Cleveland, OH), and CFU from each plate were counted. The limit of detection for the method was 100 CFU/g fecal

homogenate. For statistical purposes, plates without colonies were assigned a value of half the limit of detection, or 50 CFU/g fecal homogenate. In a separate experiment, BALB/c mice (10 per group) were fed 86-24*eae*Δ10 Str^r transformed with plasmid pEB310 (intimin-γ), plasmid pIntgbhyb (intimin hybrid), or pBlue-ScriptKS− (parent plasmid). For 10 days following infection, fecal pellets were collected and processed as described above. Fecal homogenates were plated onto sorbitol-MacConkey agar that contained streptomycin and ampicillin to select for the transformed strains. The transformed strains of EHEC O157:H7 86-24*eae*Δ10 were also plated onto sorbitol-MacConkey agar with streptomycin alone to provide an estimate of plasmid loss during infection. The data from these experiments were analyzed by a Mantel-Haenszel chi-square comparison of the proportion of mice shedding streptomycin-resistant bacteria across days. The numbers of bacteria shed by each group were compared by repeated-measures analysis of variance (ANOVA) of the logarithm of the group geometric mean of CFU from all mice in each group. For this analysis, the inoculation strain was a "between-animal factor" and day of shedding was a "within-animal factor." This statistical analysis was performed using the program SPSS (SPSS, Inc., Chicago, IL).

(ii) Infection of streptomycin-treated mice. BALB/c mice (three per group) were maintained on water supplemented with 5 g/liter of streptomycin prior to and after challenge with an inoculum of 10^8 EHEC O157:H7 86-24 Str^r or the intimin deletion strain 86-24*eae*Δ10 Str^r. Treatment with streptomycin allowed for increased colonization of the intestine in the absence of normal enteric flora (38). Three days postinoculation, mice were anesthetized via inhalation of metaphane (Schering-Plough, Kenilworth, NJ) and sacrificed by cervical dislocation. Intestines were excised from the inoculated mice and preserved in buffered formaldehyde. The portion of the large intestine adjacent to the cecum was embedded in paraffin and then sectioned onto glass slides for immunostain analysis.

Piglet and calf tissues. Formalin-fixed, paraffin-embedded spiral colon tissues were available from neonatal pigs and a neonatal calf used in earlier Shiga toxin-producing *E. coli* infection studies at the National Animal Disease Center in Ames, IA. The method for inoculation and processing of piglet and calf tissue has been described previously (6). Two cesarean-derived, colostrum-deprived, 2-day-old piglets were orally inoculated by gavage, within the first 8 h of life, with 10^6 CFU of EHEC O157:H7 strain 86-24 Str^r or 10^{10} CFU of nonpathogenic *E. coli* control strain 123 bacteria. Both were necropsied 2 days after inoculation, and intestinal samples were collected for histology. Sections from the spiral colon were used for this study. The colostrum-deprived neonatal calf (<12 h old) was inoculated with 10^{10} CFU of EHEC O157:H7 strain 86-24 Str^r, developed watery diarrhea, and was necropsied 18 h postinfection. At necropsy, intestinal samples were collected for histology (6). Sections from the distal colon were used in this study.

Western blot analysis of intimin expression. Cultures of EHEC O157:H7 86-24 Str^r strains, the intimin-negative strain 86-24*eae*Δ10 Str^r, and 86-24*eae*Δ10 Str^r complemented with plasmids pEB310, pIntgbhyb, or pBlueScriptKS were grown to mid-log phase in Luria broth at 37°C. Equivalent amounts of each bacterial culture were boiled in sample buffer that contained sodium dodecyl sulfate. The whole-cell lysates were run through a 12% polyacrylamide gel (Bio-Rad, Hercules, CA), blotted onto nitrocellulose membrane using a semidry transblot system (Bio-Rad), and blocked overnight in PBS buffer that contained 5% powdered milk (Supervalu, Inc., Eden Prairie, MN) and 0.2% Tween 20 (Sigma). Anti-intimin serum was developed in rabbits as has been described previously (36). The serum was diluted 1 part in 2,000 into the blocking solution and incubated with the nitrocellulose blot for 1 h with agitation. Unbound primary antiserum was washed from the blot with three changes of PBS, and a donkey anti-rabbit immunoglobulin G (IgG) secondary antiserum conjugated to horseradish peroxidase (Amersham, Piscataway, NJ) was diluted 1:5,000 in the blocking solution and incubated with the membrane for 1 h with agitation. Unbound antibodies were washed from the membrane with three changes of PBS. The bound antibodies were detected with an ECL Plus Western blot detection system (Amersham), and the chemiluminescent signal from the blot was recorded with a Kodak image station 440CF (Eastman Kodak, Rochester, NY).

Immunofluorescent staining. Tissue sections were deparaffinized by treatment with Histoclear (National Diagnostics, Atlanta, GA) and then rehydrated in a graded series of ethanol and water. Slides were immersed in pH 10 AntigenPlus buffer (Novagen, Madison, WI) and autoclaved at 121°C, 18 lb/in^2, for 15 min. Prior to immunostaining, tissue sections were incubated for 30 min with dilution buffer that contained 3% bovine serum albumin (Sigma) in PBS with 0.2% Tween 20 (Fisher, Fair Lawn, NJ). Anti-β1 integrin and antinucleolin sera raised in rabbits were purchased from Santa Cruz Biotechnology (Santa Cruz, CA). Rabbit anti-Tir serum was prepared as previously described (36). Normal rabbit serum obtained from animals before immunization with Tir was used as a negative control. Anti-O157 antigen typing serum was obtained from Difco. Alexa Fluor 488-labeled goat anti-rabbit IgG serum and the Zenon Alexa Fluor 555 rabbit IgG labeling kit were purchased from Molecular Probes (Eugene, OR). Anti-β1 integrin, antinucleolin, and anti-rabbit IgG sera were precleared of *E. coli*-specific antibodies by reaction with cellular proteins extracted from EHEC O157:H7. Anti-Tir pre- and postimmune sera were precleared by reaction with cellular proteins extracted from the *E. coli* K-12 expression strain BL21. All immunostaining procedures were carried out at room temperature. Primary antisera were diluted 1 part in 40 of dilution buffer and incubated on the tissue sections for 1 h, and then unbound antisera were washed from the sections with PBS. Secondary antiserum labeled with the green dye Alexa Fluor 488 was diluted 1 part in 100 of dilution buffer and incubated with the tissue sections for 1 h, and then unbound antibodies were washed from the slides with PBS. Anti-O157 serum was labeled with the red dye Zenon Alexa Fluor 555 following the manufacturer's directions. Labeled anti-O157 serum was diluted 1 part in 100 of dilution buffer and incubated with the tissue sections for 1 h, and then unbound antibodies were washed from the slides with PBS. Slides were fixed with 4% buffered formaldehyde for 20 min and then mounted with a SlowFade antifade kit (Molecular Probes). Intestinal sections from two mice, two piglets, and one calf were stained in this manner, but for consistency, only representative images of immunostained serial sections taken from single tissue blocks of an inoculated mouse, calf, and piglet are presented. An Olympus BX60 system microscope with BX-FLA reflected light fluorescence attachment was used to visualize the immunostained sections. Fluorescent and phase-contrast images were captured in grayscale format with a SPOT RT charge-coupled-device digital camera made by Diagnostic Instruments, Inc. (Sterling Heights, MI). Images were processed with the public domain program ImageJ (developed at the U.S. National Institutes of Health and available on the Internet at http://rsb.info.nih.gov/ij/). Out-of-focus fluorescence signals were deconvolved from the images by using the ImageJ module DeconvolutionJ (written by N. Linnenbrügger). Images were overlaid and false-colored red and green with the program Adobe Photoshop (Adobe Systems, Inc., San Jose, CA).

Fluorescence quantization. Images of immunostained Tir, nucleolin, and β1 integrin on mouse, calf, and pig sections were quantified by using the program ImageJ to measure the sum of the digitized fluorescence intensity in areas of 1 square μm on regions of the intestinal epithelium with and without adherent bacteria. For each immunostain from all three species, measurements were obtained for 100 adherence sites taken from at least eight separate microscopic fields and compared with an equal number of sites without bacteria taken from the same images. Analysis of these measurements and presentation of the data were accomplished using the program Microsoft Excel (Microsoft Corp., Seattle, WA). The statistical significance of the difference in fluorescence intensity between sites with and without adherent bacteria was determined by a two-tailed, paired Student *t* test of the summed intensity measurements taken at equivalent regions of the same image.

RESULTS

Intimin increased the persistence of EHEC O157:H7 infection. Groups of conventional BALB/c mice were inoculated with EHEC O157:H7 86-24 Str^r (six mice) or the intimin deletion strain EHEC O157:H7 86-24*eae*Δ10 Str^r (five mice). The bacteria shed by the mice were monitored daily for the first 4 days and on 10 of the 14 subsequent days. The results are expressed as organisms per g fecal homogenate and are presented in Fig. 1A and B. The numbers of streptomycin-resistant bacteria shed by all of the mice decreased rapidly during the first 4 days following infection. At that point, four of the five mice fed the intimin-negative strain EHEC O157:H7 86-24*eae*Δ10 Str^r no longer shed detectable levels (>100 CFU/g feces) of EHEC O157:H7, and the inoculum strain was not recovered from any of these mice after day 7. In contrast, three of the six mice fed intimin-positive EHEC O157:H7 86-24 Str^r shed detectable levels of bacteria until day 10 and one mouse continued to shed detectable levels of EHEC O157:H7 for the duration of the study (Fig. 1A). A Mantel-Haenszel chi-square analysis of these data indicated that after adjusting for day, the

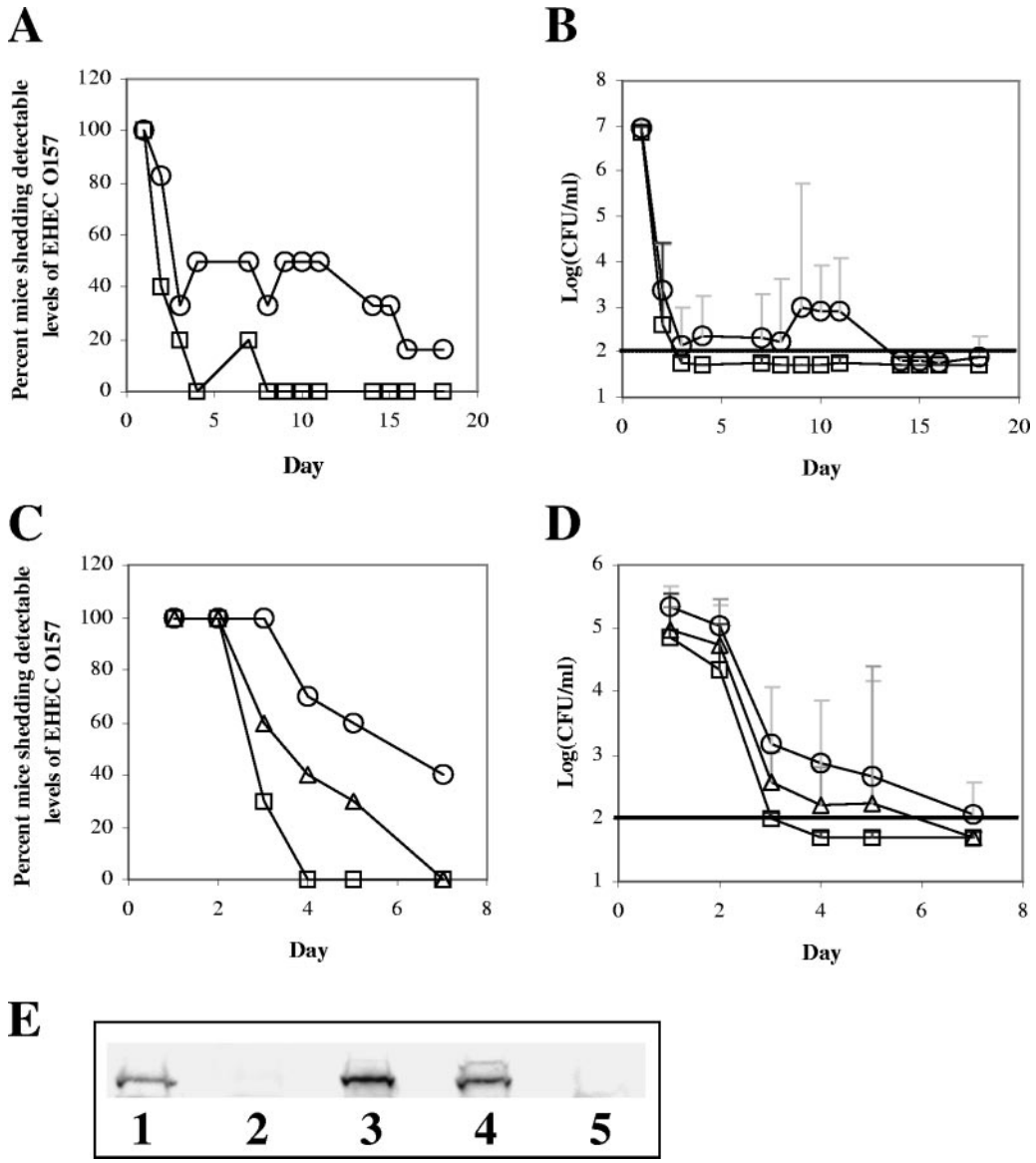

FIG. 1. EHEC O157:H7 strains that express intimin are shed by inoculated mice for longer durations than an intimin-negative strain. Female BALB/c mice were fed streptomycin-resistant EHEC O157:H7 86-24 Str^r (six mice) and intimin-negative 86-24*eae*Δ10 Str^r (five mice) strains, and fecal shedding was monitored. (A) Percentages of mice that shed strain 86-24 Str^r (circles) or strain 86-24*eae*Δ10 Str^r (squares) are presented as a function of days postinfection (*x* axis). (B) Group geometric mean of CFU per gram of feces is shown for strain 86-24 Str^r (circles) or strain 86-24*eae*Δ10 Str^r (squares). Groups of 10 female BALB/c mice were fed one of three EHEC O157:H7 86-24*eae*Δ10 Str^r isolates that had been separately transformed with plasmids that carried the gene for EHEC intimin-γ, an intimin hybrid of types γ and β, or the vector alone. For 1 week postinfection, fecal pellets were collected and processed. (C) Percentages of mice that shed EHEC O157:H7 86-24*eae*Δ10 Str^r that produced intimin-γ (circles), intimin-γβ hybrid (triangles), or no intimin (squares) are shown. (D) Group geometric mean CFU/g feces for EHEC O157:H7 86-24*eae*Δ10 Str^r that produced intimin-γ (circles), intimin-γβ hybrid (triangles), or no intimin (squares) is shown. Error bars in panels B and D represent the 95% confidence intervals of the means. Solid horizontal lines represent the limit of detection for the experiments. (E) Results of anti-intimin Western blotting for whole-cell lysates of strain 86-24 Str^r (lane 1), strain 86-24*eae*Δ10 Str^r (lane 2), and strain 86-24*eae*Δ10 Str^r transformed with the plasmids that carried the genes for intimin-γ (lane 3) or intimin-γβ hybrid (lane 4) or the control plasmid without the intimin gene (lane 5).

proportion of mice that shed streptomycin-resistant bacteria was significantly greater for the intimin-positive strain ($P < 0.0001$). The logarithm of the group geometric mean for the number of streptomycin-resistant bacteria shed by each mouse is presented in Fig. 1B. A repeated-measures ANOVA of these data that accounted for bacterial strain, day, and amount of shedding indicated that differences between the intimin-positive and intimin-negative strains were significant only on days 9, 10, and 11 after inoculation ($P < 0.01$). Twenty-three days postinoculation, the mice from both groups were sacrificed; the entire intestines and contents were homogenized in sterile PBS, and the homogenized tissues were plated onto sorbitol-MacConkey agar with streptomycin. Intimin-positive EHEC O157:H7 86-24 Str^r was recovered from the intestines of three

of six mice inoculated with that strain, while no streptomycin-resistant bacteria were detected in the intestinal homogenates of the five mice fed intimin-negative EHEC O157:H7 86-24*eae*Δ10 Str^r. Taken together, these results confirm and extend previously published findings from this laboratory that demonstrate the importance of intimin to sustained infection by EHEC O157:H7 of the murine intestine (24).

Exchange of intimin type did not increase the level of EHEC O157:H7 adherence. Groups of 10 BALB/c mice were fed EHEC O157:H7 86-24*eae*Δ10 Str^r strains that had been transformed with plasmids that expressed EHEC O157:H7 intimin, a hybrid intimin with the extracellular host cell binding domain of intimin-β from *C. rodentium*, or an empty vector without the intimin gene. Levels of infection were estimated as before by monitoring antibiotic-resistant bacteria in fecal homogenates. Fecal homogenates were plated onto agar that contained streptomycin with and without ampicillin to monitor retention of the plasmids that conferred ampicillin resistance on the bacterial strains. In all three groups, numbers of bacteria observed on plates that contained only streptomycin were similar to numbers on plates that contained both antibiotics, a finding that suggested that most of the shed bacteria retained the plasmids that were present in the original inoculum. The daily proportion of mice that shed each transformed strain is presented in Fig. 1C. The Mantel-Haenszel chi-square comparison of these data indicated that the proportion of mice that shed intimin-producing bacteria was significantly greater than the proportion that shed the strain without intimin ($P < 0.001$), while there was no significant difference between amounts of shedding of the intimin-producing strains ($P = 0.719$). The logarithm of the group geometric mean for the number of streptomycin-resistant bacteria shed by each mouse is presented in Fig. 1D. The repeated-measures ANOVA of these data revealed that while there was a difference between shedding of the strain that produced intimin-γ and shedding of the strain without intimin on days 3, 4, and 5 postinfection ($P < 0.01$), there was no significant difference on any day between the amounts of shedding of the hybrid intimin-producing strain and the intimin-negative strain ($P = 0.089$). This latter observation indicates that the hybrid intimin did not promote colonization of EHEC O157:H7 86-24*eae*Δ10 Str^r in the mouse intestine as well as did the wild-type, full-length intimin-γ. Conversely, in vitro tissue culture assays demonstrated that there was no discernible difference in the numbers of bacteria that adhered to HEp-2 cells for EHEC O157:H7 86-24*eae*Δ10 Str^r that produced the hybrid intimin compared with the strain that produced intimin-γ (data not shown). A Western blot analysis of intimin expression (Fig. 1E) showed that 86-24*eae*Δ10 Str^r complemented with the gene for wild-type intimin-γ or the gene for the hybrid intimin produced amounts of intimin that were comparable with those produced by strain 86-24 Str^r.

EHEC O157:H7 intimin deletion strain exhibited altered adherence to the intestinal epithelia of streptomycin-treated mice. To optimize the microscopic observation of EHEC O157:H7 in intestinal sections, BALB/c mice were maintained on water supplemented with the antibiotic streptomycin to eliminate normal intestinal flora. Streptomycin-treated mice were then fed 10^8 CFU of EHEC O157:H7 strain 86-24 Str^r or strain 86-24*eae*Δ10 Str^r and sacrificed 3 days postinfection.

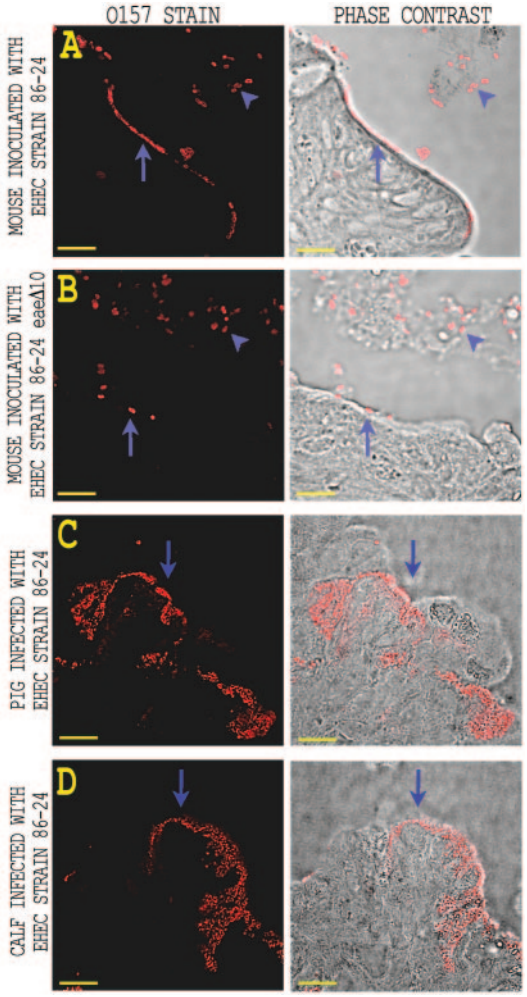

FIG. 2. Comparison of intestinal adherence patterns for animals inoculated with wild-type and intimin deletion strains of EHEC O157:H7. (A and B) Streptomycin-treated BALB/c mice were inoculated with either EHEC O157:H7 strain 86-24 Str^r or strain 86-24*eae*Δ10 Str^r. Representative fluorescent images of immunostained EHEC O157:H7 present in the intestinal sections are shown on the left. Phase-contrast micrographs of the tissue sections with the associated anti-O157 immunofluorescence are shown on the right. Bacteria of both strains were observed in the luminal space (arrowheads) and in contact with the intestinal epithelium (arrows). Intimin-positive EHEC O157:H7 strain 86-24 Str^r adhered to the intestine in an organized manner (A), while intimin-negative strain 86-24*eae*Δ10 Str^r appeared more random in adherence (B). (C and D) Immunofluorescent images of anti-O157-stained EHEC adherent to colonic sections taken from infected piglet (C) and calf (D). The bacteria are observed to be attached to the epithelial surface (arrows) in an organized manner characteristic of the A/E lesion. Bar, 10 μm.

Intestinal sections were obtained and processed, and inoculated bacteria in the intestinal sections were visualized by red-dye-labeled anti-O157:H7 typing serum as detailed in Materials and Methods. Representative images from this immunostaining procedure are shown in Fig. 2. Sections of the large intestine proximal to the cecum from mice inoculated with intimin-positive EHEC O157:H7 strain 86-24 Str^r displayed regions on the luminal surface of the epithelium in which distinct colonies of a single layer of regularly spaced EHEC

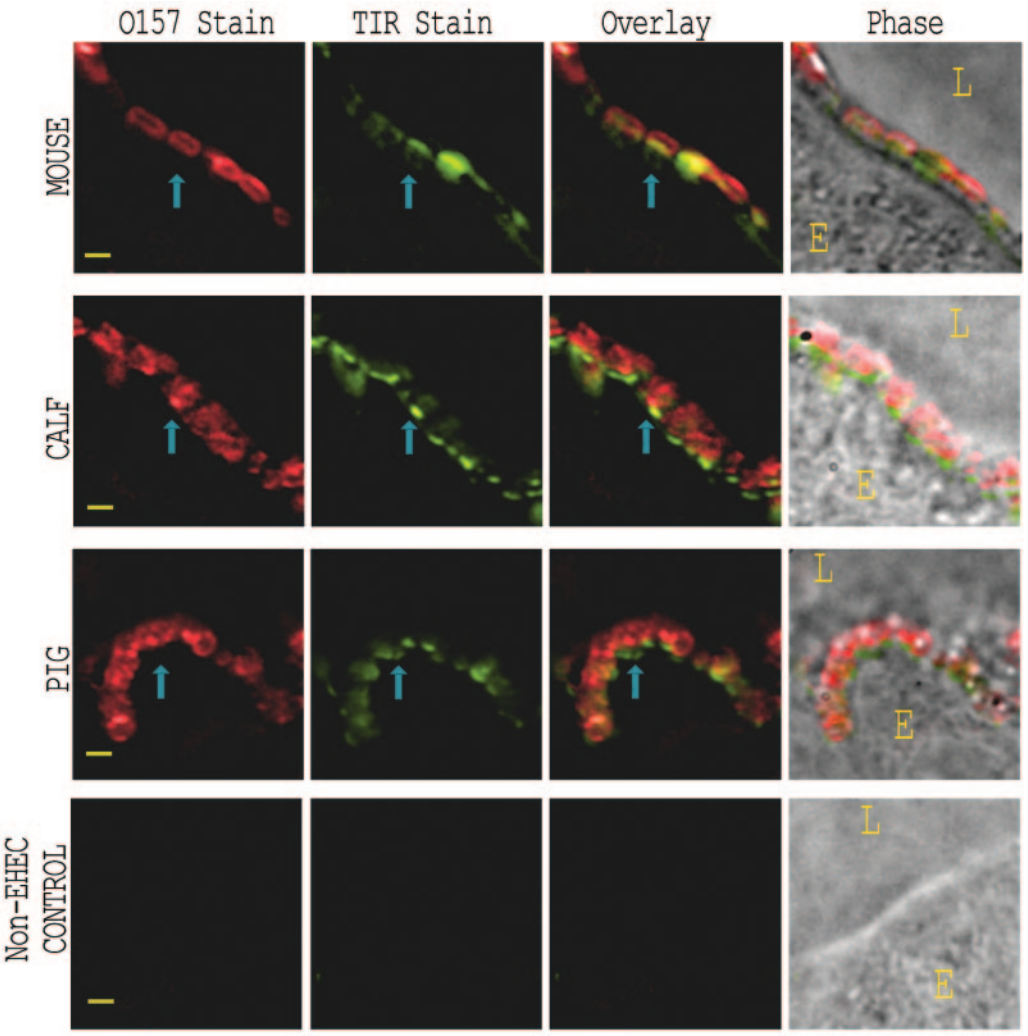

FIG. 3. Tir localization with EHEC O157:H7 on infected tissue sections, as detected by immunofluorescence. Streptomycin-treated mouse, cesarean-derived/colostrum-deprived piglet, and neonatal calf were fed EHEC O157:H7 strain 86-24 Str^r. Sections of infected intestine were immunostained with anti-Tir and anti-O157 antisera. Representative images from EHEC O157:H7-infected mouse (top row), calf (second row), and pig (third row) are shown for stained O157 (first column) and stained Tir (second column). Images in the bottom row were taken from a piglet infected with normal enteric *E. coli* strain 123. Immunostaining patterns for O157 and Tir were overlaid (third column) to demonstrate the correlation between bacteria and Tir. Phase-contrast micrographs overlaid with the combined fluorescence (fourth column) depict the orientation of the epithelial cell (E) and lumen (L). Representative adherent bacteria and associated immunostained Tir are indicated by blue arrows. Bar, 1 μm.

O157:H7 appeared to be in direct contact with epithelial cells. By contrast, no regions of organized EHEC O157:H7 adherence were evident with anti-O157-stained intestinal sections from mice inoculated with the intimin deletion strain 86-24*eae*Δ10 Str^r (Fig. 2B). Rather, intimin-negative bacteria that were in direct contact with the epithelium were generally found to occur singularly or in small clumps. There also appeared to be fewer intimin-negative bacteria closely associated with the epithelium than in the wild-type strain. Bacteria of both strains were also found in the luminal space unassociated with the epithelium (Fig. 2A and B). Few anti-O157-stained bacteria of either strain were found in sections taken from the distal large intestine (data not shown). The pattern of adherence of EHEC O157:H7 strain 86-24 Str^r to mouse epithelium was qualitatively similar to that seen for wild-type strain 86-24 in sections from pig and calf intestinal epithelium (Fig. 2C and D), but the colonies observed with pig and calf intestine appeared larger and more invaginated than the colonized regions in the mouse intestine.

Immunostained Tir was observed at the site of bacterial adherence. Intestinal sections from EHEC O157:H7 strain 86-24 Str^r-inoculated streptomycin-treated mice, neonatal calf, and neonatal piglets were stained with primary anti-Tir serum followed with a green-dye-labeled anti-rabbit IgG. Adherent EHEC O157:H7 was stained with red-dye-labeled anti-O157 typing serum. Representative results of this immunostaining are depicted in Fig. 3. Immunostained Tir was observed in the luminal intestinal epithelium adjacent to the site of EHEC O157:H7 adherence. This juxtaposition of EHEC O157:H7 and Tir staining was most apparent when the two patterns were overlaid, i.e., proximity of the staining patterns was observed at sites where bacteria touched the epithelium. Anti-Tir immu-

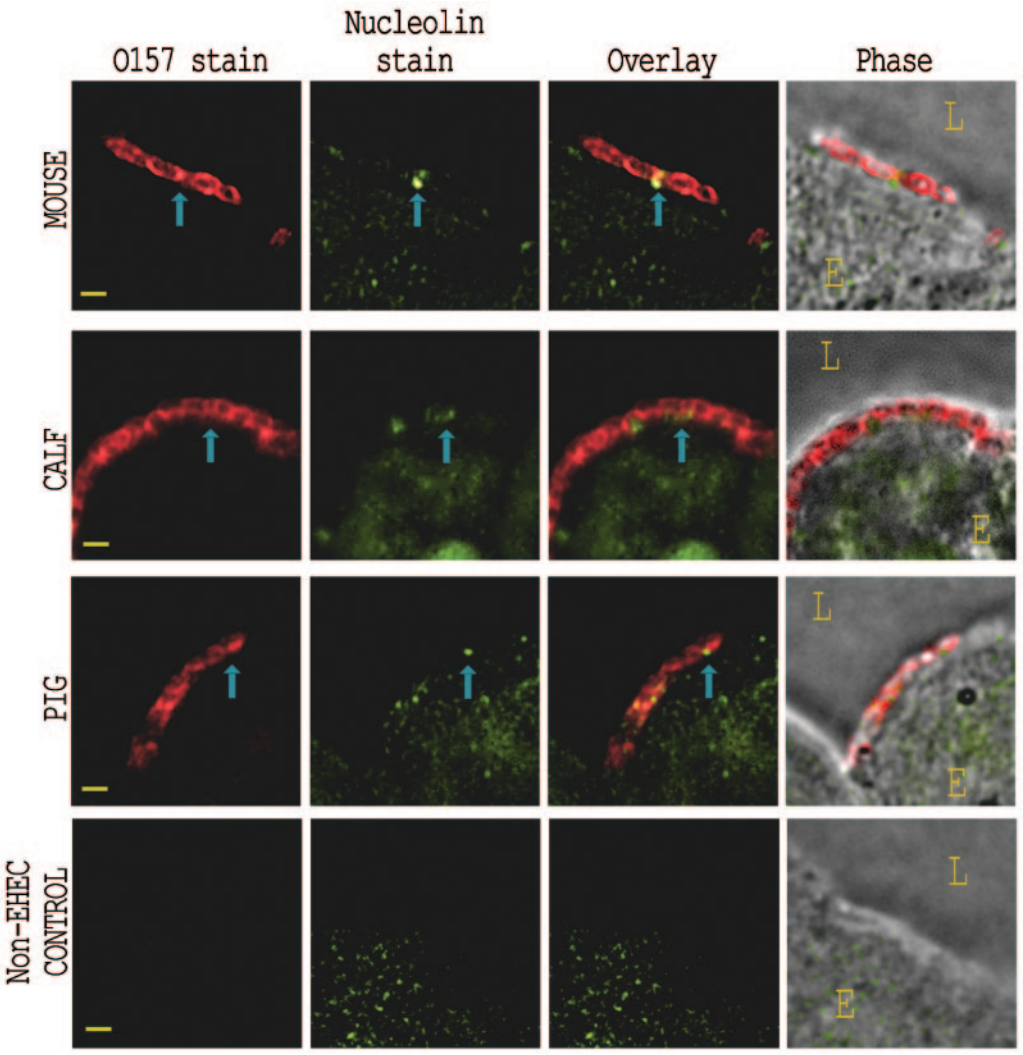

FIG. 4. Nucleolin localization with EHEC O157:H7, detected by immunofluorescence on infected tissue sections. Sections of EHEC O157:H7 Str^r-infected intestine corresponding to those depicted in Fig. 3 were immunostained with anti-nucleolin and anti-O157 sera. Representative images from EHEC O157:H7-infected mouse (top row), calf (second row), and pig (third row) are shown for stained O157 (first column) and stained nucleolin (second column). Images in the bottom row were taken from a piglet infected with the normal enteric *E. coli* strain 123. These fluorescent images were overlaid (third column) to demonstrate immunostained nucleolin around the site of bacterial adherence. Phase-contrast micrographs overlaid with the combined fluorescence (fourth column) depict the orientation of the epithelial cell (E) and lumen (L). Representative adherent bacteria and associated immunostained nucleolin are indicated by blue arrows. Bar, 1 μm.

nostain was not observed in regions of infected epithelium devoid of anti-O157-stained bacteria or in sections from the piglet inoculated with the *E. coli* control strain 123 (Fig. 3, bottom row). For all three animal types, intestinal sections reacted with preimmune normal rabbit serum showed minimal background immunofluorescence (data not shown). A quantitative analysis of the anti-Tir immunostaining patterns (see Fig. 6A) demonstrated that there was a significant increase ($P < 0.001$) in Tir immunostain at positions of bacterial adherence in intestinal sections from all three species.

Immunostained nucleolin was observed adjacent to adherent bacteria. Mouse, calf, and piglet intestinal sections from the same tissue blocks as described above were stained green with anti-nucleolin and red with anti-O157 as described above. Representative results are presented in Fig. 4. Stained nucleolin was observed in a punctate distribution in the nucleus, cytoplasm, and plasma membrane of the intestinal epithelial cells. These levels of distribution were qualitatively similar for EHEC O157:H7-infected and uninfected tissue. Immunostained bacteria were generally found attached to the epithelium at sites that were also stained for nucleolin. In mouse and pig tissue, there was minimal overlap between bacteria and stained nucleolin, but nucleolin stain did appear around and between most adherent bacteria, as was most evident in the overlaid staining patterns. In calf tissue (Fig. 4, second row), stained nucleolin appeared clustered at the site of bacterial adherence in some instances, though this pattern was not seen with all bacteria. Although surface-expressed nucleolin stain was discernible in epithelial cells from control animals not inoculated with EHEC O157:H7 (see Fig. 4, bottom row, for

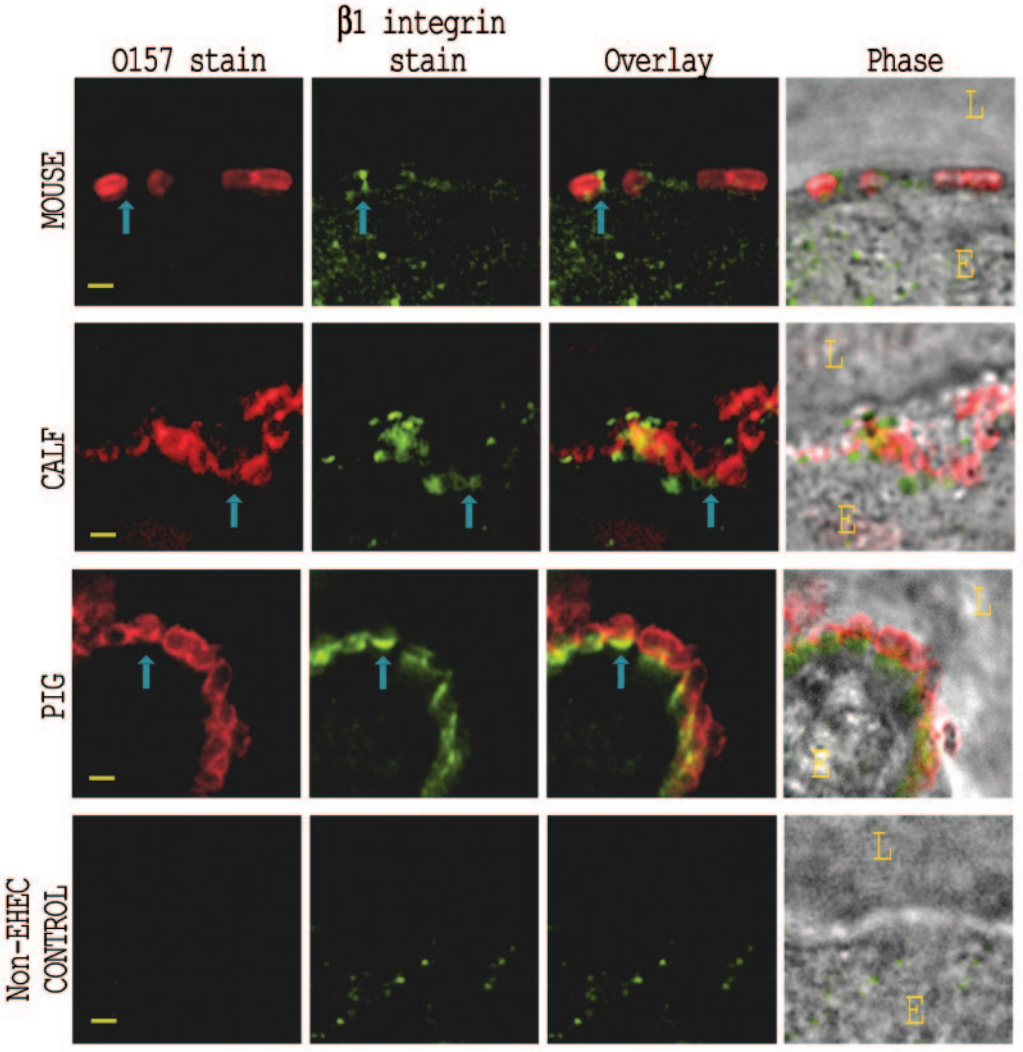

FIG. 5. β1 integrin localization with EHEC O157:H7, detected by immunofluorescence of infected tissue sections. Sections of EHEC O157:H7 Str^r-infected intestine corresponding to those depicted in Fig. 3 and 4 were immunostained with anti-β1 integrin and anti-O157 antisera. Images for mouse (top row), calf (second row), and pig (third row) are shown for stained O157 (first column) and stained β1 integrin (second column). Images in the bottom row were taken from a piglet infected with the normal enteric *E. coli* strain 123. The fluorescent images were overlaid (third column) to demonstrate accumulated β1 integrin at the site of EHEC O157:H7 adherence. Phase-contrast micrographs overlaid with the combined fluorescent images (fourth column) depict the orientation of the epithelial cell (E) and lumen (L). Representative adherent bacteria and associated immunostained β1 integrin are indicated by blue arrows. Bar, 1 μm.

piglet intestine inoculated with *E. coli* strain 123), there appeared to be an increase in the amount of nucleolin stain on the surface of cells with adherent EHEC O157:H7. A quantitative analysis of the anti-nucleolin immunostaining patterns (see Fig. 6C) demonstrated that there was a small but measurable increase in nucleolin at sites of bacterial adherence compared with equivalent epithelial regions without bacteria. The correlation between increased nucleolin immunostain and bacterial adherence was statistically significant for calf ($P = 0.028$) and pig ($P = 0.025$) intestine but was not for mouse intestine ($P = 0.097$). This increased nucleolin localized at sites of bacterial adherence could reflect tissue damage at those infection sites that resulted in the release of intranuclear nucleolin.

Immunostained β1 integrin was observed clustered with adherent bacteria. Calf, pig, and mouse intestinal sections from the same tissue blocks as described above were stained green with anti-β1 integrin serum and red with anti-O157 serum as described above. Representative immunostaining patterns are displayed in Fig. 5. Some punctate β1 integrin stain was observed on the luminal surface of the epithelium in mouse tissue (Fig. 5, top row). In a few instances, this stain was colocalized with adherent bacteria, though there was no clear correlation between the two staining patterns. In calf and pig tissue (Fig. 5, second and third rows), stained β1 integrin was clearly clustered at the site of bacterial adherence, a distribution pattern similar to that of immunostained Tir (Fig. 3). With intestinal sections from a piglet inoculated with the normal enteric *E. coli* strain 123 (Fig. 5, bottom row), immunostained β1 integrin was rarely observed at the luminal surface of the epithelial cells. A quantitative analysis of the β1 integrin im-

munostaining (Fig. 6B), demonstrated that there was a highly significant increase in fluorescence intensity at sites of bacterial adherence in calf and pig intestine ($P < 0.001$) while there was no significant difference in staining of mouse intestine ($P = 0.059$).

DISCUSSION

In this study, we examined the distribution of putative intimin receptors at the site of EHEC O157:H7 adherence to intestinal epithelial cells in three animal species. To our knowledge, this is the first demonstration of Tir accumulation beneath adherent EHEC O157 on infected tissues from orally challenged mice, calves, and piglets. Localization of the eucaryotic intimin receptors nucleolin and β1 integrin at the site of bacterial adherence in vivo represents a novel observation. Recruitment of β1 integrin to the region of EHEC O157 pedestal formation has not been reported previously, although the absence of β1 integrin beneath adherent EPEC and EHEC has been noted in vitro (14). Human tissue culture systems have been used in most investigations of EHEC O157:H7 intimin-mediated adherence to the host cell plasma membrane. Such in vitro systems, though informative, may not fully reflect the process of adherence in vivo. Findings reported in this investigation may ultimately help to identify features of the in vitro model of EHEC infection that most accurately reflect the milieu of the animal intestine.

Although pigs and neonatal calves are well-established models of EHEC O157:H7 colonization and subsequent A/E lesion formation, we sought to broaden our opportunities to dissect such lesions by developing a small-animal/murine model for that purpose. Through EHEC O157:H7 infection of both untreated and streptomycin-treated mice, we reached three major conclusions. First, we ascertained that persistent but low-level intestinal colonization of mice by EHEC O157:H7 is intimin dependent, an assumption that supports and expands previously published data from our laboratory on shedding of intimin-positive versus intimin-negative EHEC O157:H7 by mice (24). Our earlier findings were limited to 7 days of postinoculation, while the data presented in this study extend those observations to longer periods of colonization. We surmise that the persistence in mice is analogous to colonization seen with infected cattle and sheep that sporadically shed small numbers of EHEC O157:H7 for months following the initial infection (5). Second, we determined that intimin subtype alone is not responsible for the low levels of colonization in mice inoculated with EHEC O157:H7 (24) compared to high levels of colonization with *C. rodentium* (35). Thus, replacement of the extracellular domain of EHEC intimin-γ with that of intimin-β from *C. rodentium* did not increase the level of colonization of the hybrid intimin-expressing EHEC O157:H7 compared with that of the strain that made wild-type EHEC O157:H7 intimin, though both strains expressed similar levels of intimin as demonstrated by Western blot analysis. Indeed, colonization levels were lower with the hybrid intimin (Fig. 1C and D). Third, we concluded not only that the streptomycin-treated mouse model allowed a much higher level of colonization with EHEC O157:H7 than that found in untreated animals, an observation consistent with several previous studies from our group and others (38), but also that in this model the

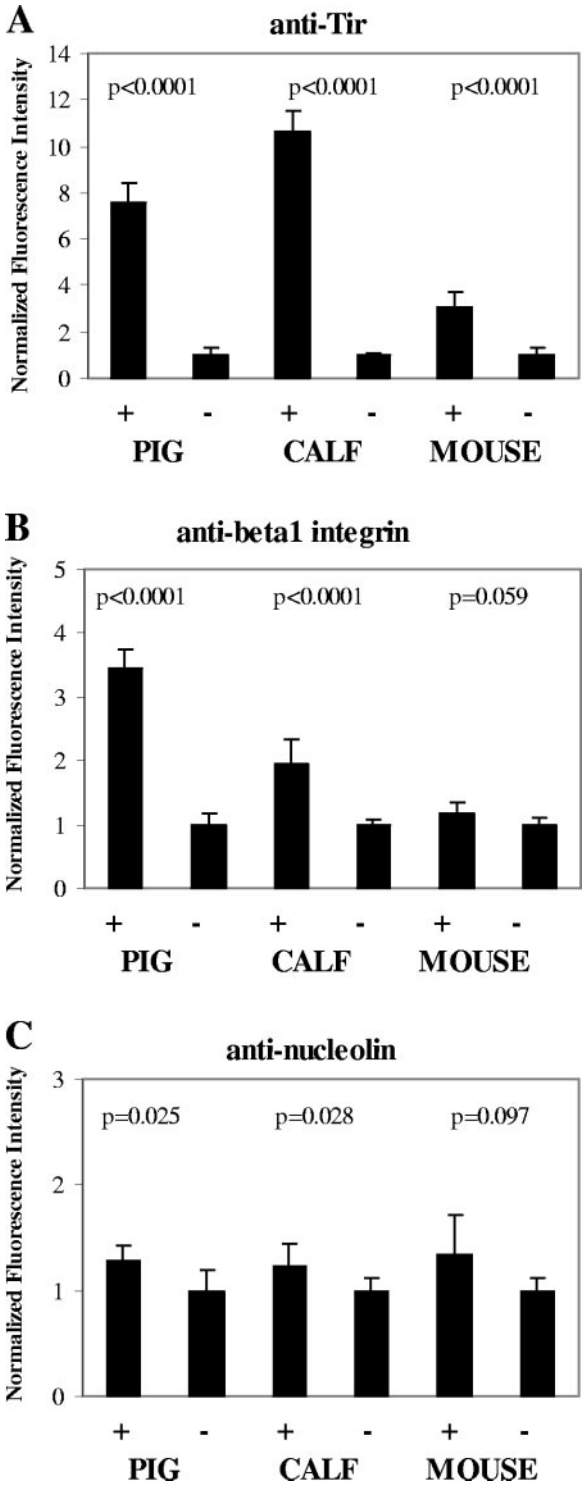

FIG. 6. Quantitative analysis of the fluorescence signal intensity obtained from digitized images of stained tissue sections. The sum of the fluorescence signal was recorded for 1 square μm at positions with (+) and without (−) adherent EHEC O157:H7 in images such as those presented in Fig. 3, 4, and 5. The solid bars represent the means of 100 observations taken from different microscopic fields of sections from pig, calf, or mouse stained for Tir (A), β1 integrin (B), or nucleolin (C). Values were normalized to the positions without adherent bacteria. Error bars represent the normalized 95% confidence intervals of the means.

pattern of bacterial adherence was different with the intimin-positive isolates versus the intimin-negative isolates (Fig. 2, compare panels A and B). In fact, the organized adherence pattern of EHEC O157:H7 86-24 Str^r to the mouse intestine was similar to the pattern seen with sections from infected calf and pig (Fig. 2, compare panel A with panels C and D). For these reasons, we considered the use of the streptomycin-treated, oral-infection mouse model to examine the distribution of EHEC O157:H7 intimin receptors at the site of bacterial attachment to be appropriate.

Our interpretation of the distribution of immunostained intimin receptors at the site of bacterial adherence on fixed tissue sections is inherently limited by the study design. While live-animal models offer advantages over in vitro tissue culture models, they may not accurately reflect the adherence process that occurs in normal animals exposed to environmental sources of EHEC O157:H7. Also, the tissue samples used in this study represent only a snapshot of the protein distribution in a single intestinal region at the instant in time that the tissues were collected and immersed in formalin. This technique is unable to convey the dynamic nature of EHEC O157:H7 adherence, in which the bacterium makes contact with the intestinal epithelium and induces a rearrangement of many host cell factors (14) to produce the actin-rich membrane extensions that partially engulf the pathogen and anchor it to the cell surface. Although we could visualize the location of putative eucaryotic intimin receptors, we could not directly examine intimin by this technique. Intimin production is reported to be down-regulated following pedestal formation (26), so that observation of intimin on adherent bacteria by immunostaining methods is difficult. For this reason, we could not determine with certainty whether intimin on the bacterial surface had interacted with any of the putative intimin receptors that were observed by immunostaining at the site of bacterial adherence. Although our interpretation of the results may be limited by the method, immunostaining of fixed tissues did allow us to determine definitively whether or not these intimin receptors were present at the site of EHEC O157:H7 adherence at the time of fixation. For example, Tir was localized at the site of bacterial contact in all three species (Fig. 3). Concentration of Tir beneath adherent bacteria is characteristic of formation of actin-rich pedestals that firmly anchor the bacteria to the host epithelium. The distribution of Tir that we observed at the site of bacterial contact with the intestinal epithelial cells in the animal tissues was very similar to Tir localization described in published reports of bacteria on human cells (13).

Nucleolin immunostain was noted on the luminal surface of epithelial cells from sections with and without adherent EHEC O157:H7. This finding was expected because nucleolin is normally found distributed throughout the nucleus, cytoplasm, and membranes of all cell types. EHEC O157:H7 infection did not dramatically change the distribution of nucleolin, but there did appear to be more immunostained nucleolin in the cytoplasm and apical membrane of epithelial cells with adherent bacteria. This nucleolin-staining pattern in infected intestine might be attributed to the cell death and associated tissue damage caused by A/E lesion formation. In tissue sections from the three different animals tested in this study, most adherent EHEC O157:H7 was found associated with some amount of immunostained nucleolin on the luminal surface of the intestinal epithelium (Fig. 4), an observation that is consistent with the tissue culture model (37). We have reported for the in vitro model of adherence that nucleolin is found associated with EHEC O157:H7 attached to HEp-2 cells and that this protein appears to play a role during initial adherence of EHEC prior to Tir insertion and pedestal formation (36, 37). The distribution of stained nucleolin that we observed around adherent bacteria on intestinal sections is consistent with our hypothesis that this protein may be involved in adherence but does not accumulate beneath bacteria.

We detected immunostained β1 integrin clustered beneath adherent O157 bacteria in pig and calf intestine (Fig. 5) in a pattern that strongly resembled that seen for Tir (Fig. 3). Minimal immunostained β1 integrin was seen on the luminal surface of epithelial cells in intestinal sections of a pig not inoculated with EHEC O157:H7. The stark contrast in localization of β1 integrin at the luminal surface of the epithelium observed between cells with attached bacteria and those without strongly suggests that integrin was recruited to the actin-rich pedestal formed by these bacteria in pig and calf tissue. An absence of β1 integrin has been reported for EPEC and EHEC pedestals formed on tissue culture cells (14, 27). Our finding of integrin staining beneath adherent bacteria may indicate that EHEC O157:H7-induced cytoskeletal rearrangements in vivo are significantly different from those in vitro. The β1 integrin immunostaining was marginal at the site of bacterial adherence on the luminal surface of the mouse intestinal epithelium. The difference in integrin localization between the small- and large-animal models may correlate with the inability of EHEC O157:H7 to colonize mice in large numbers.

We conclude from these observations that the putative eucaryotic intimin receptors nucleolin and β1 integrin were present at the site of EHEC O157:H7 adherence in vivo and would be available to interact with intimin during bacterial attachment to the intestinal epithelium of the host. The distribution of these proteins and of Tir around adherent EHEC O157:H7 in pig and calf intestine strongly suggested that these molecules had interacted with the bacteria at some point during intimate attachment. These findings confirm and extend observations of EHEC O157:H7 adherence in vitro but raise the possibility that there are distinct differences between the in vivo and in vitro models of pedestal formation.

ACKNOWLEDGMENTS

We thank Cara Olsen for assistance in statistical analysis of the data and Louise Teel for careful reading of the manuscript.

This work was supported by National Institutes of Health grant AI 20148-22 (A.D.O.) and U.S. Department of Agriculture grant 58-3625-0-135 (E.A.D.-N. and A.D.O.).

REFERENCES

1. **Adu-Bobie, J., G. Frankel, C. Bain, A. G. Goncalves, L. R. Trabulsi, G. Douce, S. Knutton, and G. Dougan.** 1998. Detection of intimins alpha, beta, gamma, and delta, four intimin derivatives expressed by attaching and effacing microbial pathogens. J. Clin. Microbiol. **36:**662–668.
2. **Barrett, T. J., J. B. Kaper, A. E. Jerse, and I. K. Wachsmuth.** 1992. Virulence factors in Shiga-like toxin-producing *Escherichia coli* isolated from humans and cattle. J. Infect. Dis. **165:**979–980.
3. **Beaudry, M., C. Zhu, J. M. Fairbrother, and J. Harel.** 1996. Genotypic and phenotypic characterization of *Escherichia coli* isolates from dogs manifesting attaching and effacing lesions. J. Clin. Microbiol. **34:**144–148.
4. **Blanco, M., J. E. Blanco, A. Mora, G. Dahbi, M. P. Alonso, E. A. González, M. I. Bernárdez, and J. Blanco.** 2004. Serotypes, virulence genes, and intimin

types of Shiga toxin (verotoxin)-producing *Escherichia coli* isolates from cattle in Spain and identification of a new intimin variant gene (*eae*ξ). J. Clin. Microbiol. **42:**645–651.
5. **Cornick, N. A., S. L. Booher, and H. W. Moon.** 2002. Intimin facilitates colonization by *Escherichia coli* O157:H7 in adult ruminants. Infect. Immun. **70:**2704–2707.
6. **Dean-Nystrom, E. A., B. T. Bosworth, H. W. Moon, and A. D. O'Brien.** 1998. *Escherichia coli* O157:H7 requires intimin for enteropathogenicity in calves. Infect. Immun. **66:**4560–4563.
7. **Dean-Nystrom, E. A., L. J. Gansheroff, M. Mills, H. W. Moon, and A. D. O'Brien.** 2002. Vaccination of pregnant dams with intimin $_{O157}$ protects suckling piglets from *Escherichia coli* O157:H7 infection. Infect. Immun. **70:**2414–2418.
8. **Deng, W., B. A. Vallance, Y. Li, J. L. Puente, and B. B. Finlay.** 2003. *Citrobacter rodentium* translocated intimin receptor (Tir) is an essential virulence factor needed for actin condensation, intestinal colonization and colonic hyperplasia in mice. Mol. Microbiol. **48:**95–115.
9. **Donnenberg, M. S., S. Tzipori, M. L. McKee, A. D. O'Brien, J. Alroy, and J. B. Kaper.** 1993. The role of the *eae* gene of enterohemorrhagic *Escherichia coli* in intimate attachment *in vitro* and in a porcine model. J. Clin. Investig. **92:**1418–1424.
10. **Frankel, G., O. Lider, R. Hershkoviz, A. P. Mould, S. G. Kachalsky, D. C. Candy, L. Cahalon, M. J. Humphries, and G. Dougan.** 1996. The cell-binding domain of intimin from enteropathogenic *Escherichia coli* binds to beta1 integrins. J. Biol. Chem. **271:**20359–20364.
11. **Frankel, G., A. D. Phillips, L. R. Trabulsi, S. Knutton, G. Dougan, and S. Matthews.** 2001. Intimin and the host cell—is it bound to end in Tir(s)? Trends Microbiol. **9:**214–218.
12. **Gansheroff, L. J., M. R. Wachtel, and A. D. O'Brien.** 1999. Decreased adherence of enterohemorrhagic *Escherichia coli* to HEp-2 cells in the presence of antibodies that recognize the C-terminal region of intimin. Infect. Immun. **67:**6409–6417.
13. **Goosney, D. L., M. de Grado, and B. B. Finlay.** 1999. Putting *E. coli* on a pedestal: a unique system to study signal transduction and the actin cytoskeleton. Trends Cell Biol. **9:**11–14.
14. **Goosney, D. L., R. DeVinney, and B. B. Finlay.** 2001. Recruitment of cytoskeletal and signaling proteins to enteropathogenic and enterohemorrhagic *Escherichia coli* pedestals. Infect. Immun. **69:**3315–3322.
15. **Hartland, E. L., M. Batchelor, R. M. Delahay, C. Hale, S. Matthews, G. Dougan, S. Knutton, I. Connerton, and G. Frankel.** 1999. Binding of intimin from enteropathogenic *Escherichia coli* to Tir and to host cells. Mol. Microbiol. **32:**151–158.
16. **Hartland, E. L., V. Huter, L. M. Higgins, N. S. Goncalves, G. Dougan, A. D. Phillips, T. T. MacDonald, and G. Frankel.** 2000. Expression of intimin γ from enterohemorrhagic *Escherichia coli* in *Citrobacter rodentium*. Infect. Immun. **68:**4637–4646.
17. **Higgins, L. M., G. Frankel, I. Connerton, N. S. Goncalves, G. Dougan, and T. T. MacDonald.** 1999. Role of bacterial intimin in colonic hyperplasia and inflammation. Science **285:**588–591.
18. **Isberg, R. R., and J. M. Leong.** 1990. Multiple beta 1 chain integrins are receptors for invasin, a protein that promotes bacterial penetration into mammalian cells. Cell **60:**861–871.
19. **Isberg, R. R., D. L. Voorhis, and S. Falkow.** 1987. Identification of invasin: a protein that allows enteric bacteria to penetrate cultured mammalian cells. Cell **50:**769–778.
20. **Jarvis, K. G., J. A. Giron, A. E. Jerse, T. K. McDaniel, M. S. Donnenberg, and J. B. Kaper.** 1995. Enteropathogenic *Escherichia coli* contains a putative type III secretion system necessary for the export of proteins involved in attaching and effacing lesion formation. Proc. Natl. Acad. Sci. USA **92:**7996–8000.
21. **Jerse, A. E., and J. B. Kaper.** 1991. The *eae* gene of enteropathogenic *Escherichia coli* encodes a 94-kilodalton membrane protein, the expression of which is influenced by the EAF plasmid. Infect. Immun. **59:**4302–4309.
22. **Jerse, A. E., J. Yu, B. D. Tall, and J. B. Kaper.** 1990. A genetic locus of enteropathogenic *Escherichia coli* necessary for the production of attaching and effacing lesions on tissue culture cells. Proc. Natl. Acad. Sci. USA **87:**7839–7843.
23. **Jordan, D. M., S. L. Booher, and H. W. Moon.** 2005. *Escherichia coli* O157:H7 does not require intimin to persist in pigs. Infect. Immun. **73:**1865–1867.
24. **Judge, N. A., H. S. Mason, and A. D. O'Brien.** 2004. Plant cell-based intimin vaccine given orally to mice primed with intimin reduces time of *Escherichia coli* O157:H7 shedding in feces. Infect. Immun. **72:**168–175.
25. **Kenny, B., R. DeVinney, M. Stein, D. J. Reinscheid, E. A. Frey, and B. B. Finlay.** 1997. Enteropathogenic *E. coli* (EPEC) transfers its receptor for intimate adherence into mammalian cells. Cell **91:**511–520.
26. **Knutton, S., J. Adu-Bobie, C. Bain, A. D. Phillips, G. Dougan, and G. Frankel.** 1997. Down regulation of intimin expression during attaching and effacing enteropathogenic *Escherichia coli* adhesion. Infect. Immun. **65:**1644–1652.
27. **Liu, H., L. Magoun, and J. M. Leong.** 1999. β_1-chain integrins are not essential for intimin-mediated host cell attachment and enteropathogenic *Escherichia coli*-induced actin condensation. Infect. Immun. **67:**2045–2049.
28. **McGraw, E. A., J. Li, R. K. Selander, and T. S. Whittam.** 1999. Molecular evolution and mosaic structure of alpha, beta, and gamma intimins of pathogenic *Escherichia coli*. Mol. Biol. Evol. **16:**12–22.
29. **McKee, M. L., A. R. Melton-Celsa, R. A. Moxley, D. H. Francis, and A. D. O'Brien.** 1995. Enterohemorrhagic *Escherichia coli* O157:H7 requires intimin to colonize the gnotobiotic pig intestine and to adhere to HEp-2 cells. Infect. Immun. **63:**3739–3744.
30. **Melton-Celsa, A. R., J. E. Rogers, C. K. Schmitt, S. C. Darnell, and A. D. O'Brien.** 1998. Virulence of Shiga toxin-producing *Escherichia coli* (STEC) in orally-infected mice correlates with the type of toxin produced by the infecting strain. Jpn. J. Med. Sci. Biol. **51:**S108–S114.
31. **Neef, N. A., S. McOrist, R. J. Lysons, A. P. Bland, and B. G. Miller.** 1994. Development of large intestinal attaching and effacing lesions in pigs in association with the feeding of a particular diet. Infect. Immun. **62:**4325–4332.
32. **Ostroff, S. M., P. M. Griffin, R. V. Tauxe, L. D. Shipman, K. D. Greene, J. G. Wells, J. H. Lewis, P. A. Blake, and J. M. Kobayashi.** 1990. A statewide outbreak of *Escherichia coli* O157:H7 infections in Washington State. Am. J. Epidemiol. **132:**239–247.
33. **Phillips, A. D., and G. Frankel.** 2000. Intimin-mediated tissue specificity in enteropathogenic *Escherichia coli* interaction with human intestinal organ cultures. J. Infect. Dis. **181:**1496–1500.
34. **Phillips, A. D., J. Giron, S. Hicks, G. Dougan, and G. Frankel.** 2000. Intimin from enteropathogenic *Escherichia coli* mediates remodelling of the eukaryotic cell surface. Microbiology **146:**1333–1344.
35. **Schauer, D. B., and S. Falkow.** 1993. Attaching and effacing locus of a *Citrobacter freundii* biotype that causes transmissible murine colonic hyperplasia. Infect. Immun. **61:**2486–2492.
36. **Sinclair, J. F., and A. D. O'Brien.** 2002. Cell surface-localized nucleolin is a eukaryotic receptor for the adhesin intimin-gamma of enterohemorrhagic *Escherichia coli* O157:H7. J. Biol. Chem. **277:**2876–2885.
37. **Sinclair, J. F., and A. D. O'Brien.** 2004. Intimin types alpha, beta, and gamma bind to nucleolin with equivalent affinity but lower avidity than to the translocated intimin receptor. J. Biol. Chem. **279:**33751–33758.
38. **Wadolkowski, E. A., J. A. Burris, and A. D. O'Brien.** 1990. Mouse model for colonization and disease caused by enterohemorrhagic *Escherichia coli* O157:H7. Infect. Immun. **58:**2438–2445.
39. **Zhang, W. L., B. Kohler, E. Oswald, L. Beutin, H. Karch, S. Morabito, A. Caprioli, S. Suerbaum, and H. Schmidt.** 2002. Genetic diversity of intimin genes of attaching and effacing *Escherichia coli* strains. J. Clin. Microbiol. **40:**4486–4492.

Editor: J. T. Barbieri